Decentralized Neural Network-based Excitation Control of Large-scale Power Systems

Wenxin Liu, Jagannathan Sarangapani, Ganesh K. Venayagamoorthy, Li Liu, Donald C. Wunsch II, Mariesa L. Crow, and David A. Cartes

Abstract: This paper presents a neural network based decentralized excitation controller design for large-scale power systems. The proposed controller design considers not only the dynamics of generators but also the algebraic constraints of the power flow equations. The control signals are calculated using only local signals. The transient stability and the coordination of the subsystem control activities are guaranteed through rigorous stability analysis. Neural networks in the controller design are used to approximate the unknown/imprecise dynamics of the local power system and the interconnections. All signals in the closed loop system are guaranteed to be uniformly ultimately bounded. To evaluate its performance, the proposed controller design is compared with conventional controllers optimized using particle swarm optimization. Simulations with a three-machine power system under different disturbances demonstrate the effectiveness of the proposed controller design.

Keywords: Decentralized control, large-scale system, neural networks, power system control.

1. INTRODUCTION

Power systems are large-scale, distributed and highly nonlinear with fast transients. To coordinate the control activities of the overall system, centralized control schemes are proposed by assuming that global information of the entire system is available. However, centralized controllers are very difficult to design and implement for complex large-scale systems due to technical and economic reasons. Furthermore, centralized controller designs are dependent upon the system structure and cannot handle the structural changes.

Decentralized control schemes are proposed to overcome these problems of centralized control. Instead of designing a global central controller, decentralized controller design aims at designing separate local controllers for each subsystem. The subsystem controllers require only local signals and/or a minimum amount of information from other subsystems.

Traditionally, the decentralized control strategies of power systems were designed based on linearized system models at certain operating points. The selection of operating points and tuning of parameters are quite empirical. Moreover, the performance of these controllers cannot be guaranteed under certain unforeseen large disturbances.

With the introduction of differential geometric methods, various stabilizing control results are reported based on nonlinear multimachine power system models [1,2]. However, differential geometric based nonlinear controller designs require exact knowledge of system dynamics. Imprecise knowledge will degrade the performance of the controller designs. Since it is impossible to make the assumption that the complex power system dynamics can be known accurately, these controller designs cannot be widely accepted.

In order to overcome the limitation of the methods mentioned above, and to enhance the robustness of the power system, numerous results on the decentralized nonlinear robust control of power systems have appeared [3-10]. Some model uncertainties are considered, even though most of the controller designs are still based on the differential geometric or backstepping methodologies. In all these papers, the stability and robustness of the control system were demonstrated using Lyapunov analysis.

Neural networks have been proven an excellent tool for function approximation and therefore they are used to approximate nonlinear systems. Recently,

Manuscript received February 2, 2006; revised May 19, 2007; accepted June 28, 2007. Recommended by Editor Jin Young Choi.

Wenxin Liu, Li Liu, and Dave A. Cartes are with the Center for Advanced Power Systems, Florida State University, 2000 Levy Ave, Tallahassee, 32310, USA (e-mails: {wliu, lliu, dave}@caps.fsu.edu).

Jagannathan Sarangapani, Ganesh K. Venayagamoorthy, Donald C. Wunsch II, and Mariesa L. Crow are with the Department of Electrical and Computer Engineering, University of Missouri - Rolla, MO 65401 USA (e-mails: {sarangap, ganeshv, dwunsch, crow}@umr.edu).

Neural Networks (NN) were applied to the design of decentralized controllers [11,12]. In these papers, NNs are used to approximate the unknown nonlinear dynamics of the subsystems and to compensate the unknown nonlinear interactions. Though local measured information is used in the controller design of subsystems, the coordination of subsystem controllers and the transient performance can be guaranteed. These designs are applicable to a limited class of nonlinear systems. In [13], a decentralized neural network control scheme was proposed for a class of nonlinear systems that does not satisfy the matching conditions.

The proposed work extends the authors' previous work on indirect [14,15] and direct [16-18] NN-based power systems controls to the decentralized control of large-scale power systems described by Differential Algebraic Equations (DAE). In the DAE model, the differential equations are used to model the dynamics of the generators, and the algebraic equations are used to model the power flow constraints. Before the controller design, the algebraic equations are first transformed into differential equations based on circuit theory. After that, bounds of the interconnection terms are analyzed for the transformed model. Subsequently, NN-based decentralized controller design is presented. It can be concluded that all the signals in the closed loop are uniformly ultimately bounded.

To evaluate its performance, the proposed controller design is compared with conventional excitation controls including an Automatic Voltage Regulator (AVR) and a Conventional Power System Stabilizer (CPSS). It is well known that it is a difficult job to tune the design parameters of the conventional controls especially for large-scale power systems. Particle Swarm Optimization (PSO) is applied to optimize the parameters tuning process. The proposed controller design is then compared with the best possible performance of the conventional controllers. Simulations with the WECC 3-machine 9-bus power system demonstrate the effectiveness of the proposed controller design.

The rest of the paper is organized as follows. Section 2 briefly introduces the approximation property of NN and stability of nonlinear system. Section 3 presents the model transformation, and bound analysis. The decentralized neural network controller design is presented in Section 4. Simulation results are provided in Section 5, and finally, conclusion is given in Section 6.

2. BACKGROUND

The following mathematical notions are required for system approximation using NNs and stability analysis for the design of an adaptive NN controller.

2.1. Approximation property of NN

The commonly used property of NN for control is its function approximation and adaptation capability [19]. Let $f(x)$ be a smooth function from $R^n \rightarrow R^m$, then it can be shown that, as long as x is restricted to a compact set $S \in R^n$, for some sufficiently large number of hidden-layer neurons, there exist a set of weights and thresholds such that

$$f(x) = W^T \varphi(x) + \varepsilon(x), \tag{1}$$

where x is the input vector, $\varphi(.)$ is the activation function, W is the weight matrix of the output layer, and $\varepsilon(x)$ is the approximation error. Equation (1) indicates that a NN can approximate any continuous function in a compact set. In fact, for any choice of a positive number ε_N, one can find a NN such that $\varepsilon(x) \leq \varepsilon_N$ for all $x \in S$. For suitable function approximation, φ(x) must form a basis [20].

For a two layer NN, $\varphi(x)$ is defined as $\varphi(x)=\sigma(V^T x)$, where V is the weight matrix of the first layer, and $\sigma(x)$ is the sigmoid function. If V is fixed, then the only design parameter in the NN is W matrix, and this NN becomes a simplified version of function link network (one layer NN), which is easier to train. It has been shown in [21] that $\varphi(x)$ can form a basis if V is chosen randomly. The larger the number of the hidden layer neurons N_h is, the smaller is the approximation error $\varepsilon(x)$. Baron shows that the NN approximation error $\varepsilon(x)$ for one layer NN is fundamentally bounded by a term of the order $(1/n)^{2/d}$, where n is the number of fixed basis functions, and d is the dimension of the input to the NN [19].

2.2. Stability of systems

Consider the nonlinear system given by

$$\begin{aligned} \dot{x} &= f(x,u), \\ y &= h(x), \end{aligned} \tag{2}$$

where $x(t)$ is a state vector, $u(t)$ is the input vector, and $y(t)$ is the output vector [22]. The solution to (2) is uniformly ultimately bounded (UUB) if for any U, a compact subset of R_n, and all $x(t_0) = x_0 \in U$ there exists an $\varepsilon>0$, and a number $T(\varepsilon,x_0)$ such that $\|x(t)\|<\varepsilon$ for all $t \geq t_0+T$.

3. POWER SYSTEM MODEL TRANSFORMATION AND BOUND ANALYSIS

Large-scale power systems can be represented using Differential Algebraic Equations (DAE) [23]. The differential and algebraic equations represent the generator dynamics, and power flow constraints, respectively.

$$\begin{cases} \dfrac{d\delta_i}{dt} = \omega_i - \omega_s \\ \dfrac{2H_i}{\omega_s}\dfrac{d\omega_i}{dt} = T_{mi} - E'_{qi}I_{qi} - (X_{qi} - X'_{di})I_{di}I_{qi} \\ T'_{d0i}\dfrac{dE'_{qi}}{dt} = -E'_{qi} - (X_{di} - X'_{di})I_{di} + E_{fdi}, \end{cases} \quad (3)$$

and

$$\begin{cases} 0 = P_i^{inj} - V_i \sum_{j=1}^{N} V_j Y_{ij} \cos(\theta_i - \theta_j - \phi_{ij}) \\ 0 = Q_i^{inj} - V_i \sum_{j=1}^{N} V_j Y_{ij} \sin(\theta_i - \theta_j - \phi_{ij}), \end{cases} \quad (4)$$

where I_{di} and I_{qi} satisfy the following equations.

$$\begin{cases} V_i \sin(\delta_i - \theta_i) - X_{qi}I_{qi} = 0 \\ V_i \cos(\delta_i - \theta_i) + X'_{di}I_{di} - E'_{qi} = 0 \end{cases} \quad (5)$$

In (3)-(5), i=1,2,…,n; n is the number of generators/ subsystems; N is the number of the buses; δ_i is the power angle of the i^{th} generator in rad; ω_i is the rotating speed of the i^{th} generator in rad/s; ω_s is the synchronous machine rotating speed in rad/s; H_i is the inertia constant in seconds; T_{mi} is the mechanical input power in *p.u.*; E'_{qi} is the q-axis internal transient electric potential of the i^{th} generator in *p.u.*; E_{fdi} is the control signal in *p.u.*; P_i^{inj} and Q_i^{inh} are the injected active and reactive power at bus i in *p.u.*; $V_i\angle\theta_i$ is the voltage at bus i; and $Y_{ij}\angle\phi_{ij}$ is admittance between bus i and bus j.

The difficulty encountered during the controller design for the above DAE based model is the manipulation of algebraic constraints. According to (5), we can see that I_{di} and I_{qi} in (3) are functions of local measured variables δ_i and $V_i\angle\theta_i$. Since $V_i\angle\theta_i$ is subjected to algebraic equation constraints (4), I_{di} and I_{qi} can be expressed as a function of the states of the differential equations only. This procedure is discussed next.

According to circuit theory, the voltages and injected currents at the generator buses satisfy the following equation:

$$\bar{V} = Z_{bus}\bar{I}, \quad (6)$$

where $\bar{V} = [V_1,...V_n]^T$ and $\bar{I} = [I_1,...I_n]^T$ are all $n\times 1$ vectors, $Z_{bus} = R + jX$ is a $n\times n$ matrix of the equivalent impedance of the network.

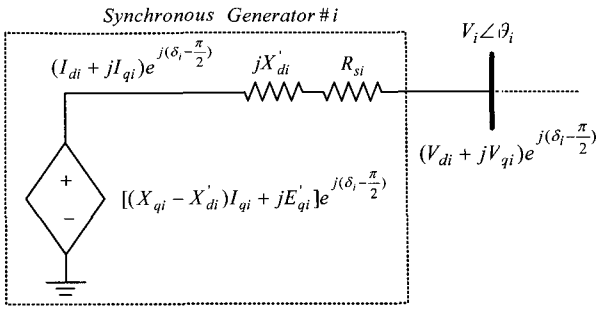

Fig. 1. Dynamic circuit of the synchronous generator.

The dynamic circuit of the synchronous generator can be represented by the following figure [23].

According to Fig. 1, we have

$$\bar{I} = (I_d + jI_q).e^{j(\delta-\frac{\pi}{2})} \quad (7)$$

and

$$\bar{V} = [(X_q.I_q - R_s.I_d) + j(E'_q - X'_d.I_d - R_s.I_q)].e^{j(\delta-\frac{\pi}{2})}, \quad (8)$$

where $I_d = [I_{d1},...I_{dn}]^T$, $I_q = [I_{q1},...I_{qn}]^T$, $\delta = [\delta_1, ...\delta_n]^T$, $X_q = [X_{q1},...X_{qn}]^T$, $X'_d = [X'_{d1},...X'_{dn}]^T$, $E'_q = [E'_{q1},...E'_{qn}]^T$, and $R_s = [R_{s1},...R_{sn}]^T$ are all $n\times 1$ vectors, "." denotes "dot multiplication".

Since R_s elements are usually very small, R_s can be assumed as a null vector. Substituting (7) and (8) into (5), one can get

$$[X_q.I_q + j(E'_q - X'_d.I_d].e^{j(\delta-\frac{\pi}{2})} = (R + jX)[(I_d + jI_q).e^{j(\delta-\frac{\pi}{2})}]. \quad (9)$$

That is

$$\begin{cases} X_q.I_q.\sin\delta + (E'_q - X'_d.I_d).\cos\delta \\ \quad = R(I_d.\sin\delta + I_q.\cos\delta) - X(I_q.\sin\delta - I_d.\cos\delta) \\ (E'_q - X'_d.I_d).\sin\delta - X_q.I_q.\cos\delta \\ \quad = R(I_q.\sin\delta - I_d.\cos\delta) + X(I_d.\sin\delta + I_q.\cos\delta). \end{cases} \quad (10)$$

Considering the i^{th} elements of the above equations, we get

$$\begin{cases} E'_{qi}\cos\delta_i = \sum_{j=1}^{n} \begin{Bmatrix} [R_{ij}\sin\delta_j + (A_{ij} + X_{ij})\cos\delta_j]I_{dj} \\ +[-(B_{ij} + X_{ij})\sin\delta_j + R_{ij}\cos\delta_j]I_{qj} \end{Bmatrix} \\ E'_{qi}\sin\delta_i = \sum_{j=1}^{n} \begin{Bmatrix} [(A_{ij} + X_{ij})\sin\delta_j - R_{ij}\cos\delta_j]I_{dj} \\ +[R_{ij}\sin\delta_j + (B_{ij} + X_{ij})\cos\delta_j]I_{qj} \end{Bmatrix}, \end{cases} \quad (11)$$

where R_{ij} and X_{ij} are the i,j-th element of matrix R and X respectively, and A and $B$are defined according to $A = diag[X'_{d1},...,X'_{dn}]$ and $B = diag[X_{q1},...,X_{qn}]$.

Equation (11) can be expressed using the following equation

$$Y = MX, \tag{12}$$

where vectors X, Y and matrix M are defined as follows:

$$X = [I_{d1}, I_{q1},..., I_{di}, I_{qi},..., I_{dn}, I_{qn}]^T,$$

$$Y = [E'_{q1}\cos\delta_1, E'_{q1}\sin\delta_1, ..., E'_{qi}\cos\delta_i, E'_{qi}\sin\delta_i,..., E'_{qn}\cos\delta_n, E'_{qn}\sin\delta_n]^T,$$

$$M = \begin{bmatrix} \alpha_{11} & \beta_{11} & \cdots & \alpha_{1i} & \beta_{1i} & \cdots & \alpha_{1n} & \beta_{1n} \\ \phi_{11} & \varphi_{11} & \cdots & \phi_{1i} & \varphi_{1i} & \cdots & \phi_{1n} & \varphi_{1n} \\ \vdots & \vdots & \vdots & \vdots & \vdots & \vdots & \vdots & \vdots \\ \alpha_{i1} & \beta_{i1} & \cdots & \alpha_{ii} & \beta_{ii} & \cdots & \alpha_{in} & \beta_{in} \\ \phi_{i1} & \varphi_{i1} & \cdots & \phi_{ii} & \varphi_{ii} & \cdots & \phi_{in} & \varphi_{in} \\ \vdots & \vdots & \vdots & \vdots & \vdots & \vdots & \vdots & \vdots \\ \alpha_{n1} & \beta_{n1} & \cdots & \alpha_{ni} & \beta_{ni} & \cdots & \alpha_{nn} & \beta_{nn} \\ \phi_{n1} & \varphi_{n1} & \cdots & \phi_{ni} & \varphi_{ni} & \cdots & \phi_{nn} & \varphi_{nn} \end{bmatrix}. \tag{13}$$

The variables in M are defined according to

$$\begin{aligned} \alpha_{ij} &= M_{2i-1,2j-1} = R_{ij}\sin\delta_j + (A_{ij} + X_{ij})\cos\delta_j, \\ \beta_{ij} &= M_{2i-1,2j} = -(B_{ij} + X_{ij})\sin\delta_j + R_{ij}\cos\delta_j, \\ \phi_{ij} &= M_{2i,2j-1} = (A_{ij} + X_{ij})\sin\delta_j - R_{ij}\cos\delta_j, \\ \varphi_{ij} &= M_{2i,2j} = R_{ij}\sin\delta_j + (B_{ij} + X_{ij})\cos\delta_j. \end{aligned} \tag{14}$$

During the operation range of a power system, M should always be a full rank matrix. This is proved later during our simulation under different operating conditions. Thus the inverse matrix of M exist, and I_{di} and I_{qi} can be expressed as linear combinations of E'_{qj} with the parameters $\phi_{ij}(\bar{\delta})$ and $\psi_{ij}(\bar{\delta})$ defined as linear combinations of the $\sin\delta_i$ and $\cos\delta_i$ together with the parameters of the power systems.

$$\begin{cases} I_{di} = \sum_{j=1}^{n} \phi_{ij}(\bar{\delta}) E'_{qj} \\ I_{qi} = \sum_{j=1}^{n} \psi_{ij}(\bar{\delta}) E'_{qj}, \end{cases} \tag{15}$$

where $\bar{\delta} = [\delta_1,...,\delta_n]^T$ denote all the rotor angles.

Since the linear combination of bounded variables are always bounded, the bound of I_{di} and I_{qi} can be expressed as in (16).

$$\begin{cases} |I_{di}| \le \sum_{j=1}^{n} \Phi_{ij} |E'_{qj}| \\ |I_{qi}| \le \sum_{j=1}^{n} \Psi_{ij} |E'_{qj}|, \end{cases} \tag{16}$$

where constants Φ_{ij} and Ψ_{ij} are the bounds of $\varphi_{ij}(\delta)$ and $\psi_{ij}(\delta)$ respectively. Note that we do not need to calculate the value of Φ_{ij} and Ψ_{ij} in our calculation of control signals. We only use these expressions to analyze the bounds of the interconnection terms.

To simplify the controller design, the third system state E'_q is substituted using a measurable variable P_{ei}, and it is defined as

$$P_{ei} = E'_{qi} I_{qi} + (X_{qi} - X'_{di}) I_{di} I_{qi}. \tag{17}$$

Thus the system dynamics can be transformed into

$$\begin{aligned} \dot{\delta}_i &= \omega_i - \omega_s, \\ \dot{\omega}_i &= \frac{\omega_s}{2H_i} T_{mi} - \frac{\omega_s}{2H_i} P_{ei}, \\ \dot{P}_{ei} &= -\frac{1}{T'_{d0i}} P_{ei} + \frac{1}{T'_{d0i}} v_i + \Delta_i(.), \end{aligned} \tag{18}$$

where the virtual control signal for the transformed system is defined as

$$v_i = E_{fdi} I_{qi} = \Delta v_i + v_{i0}. \tag{19}$$

In (19), v_{i0} is the reference value of v_i, and Δv_i is the deviation of v_i from v_{i0}. $\Delta_i(.)$ is called the interconnection term and defined as [24]

$$\begin{aligned} \Delta_i(.) = {} & (X_{qi} - X_{di}) I_{di} I_{qi} + E'_{qi} \dot{I}_{qi} \\ & + (X_{qi} - X'_{di})(\dot{I}_{di} I_{qi} + I_{di} \dot{I}_{qi}). \end{aligned} \tag{20}$$

According to (19), we can calculate E_{fd} as long as I_{qi} is not zero. The term $|\Delta_i(.)|$ can be expressed as a sum of subsystem states since our controller design requires the bound on the interconnection terms. Consequently, the following assumption can be applied to obtain these bounds.

Assumption 1: The excitation voltage E_{fdi} can be at most k times as large as $E_{qi} = E'_{qi} + (X_{di} - X'_{di}) I_{di}$ [5].

The above assumption is very important to obtain the bound on the interconnection terms. According to this assumption and (16), we have

$$\left|\dot{E}_{qi}^{'}\right| = \frac{1}{T_{d0i}^{'}}\left|E_{fdi} - E_{qi}\right| \le \frac{k}{T_{d0i}^{'}}\left|E_{qi}\right|$$
$$\le \frac{k}{T_{d0i}^{'}}\left|E_{qi}^{'} + (X_{di} - X_{di}^{'})\sum_{j=1}^{n}\phi_{ij}(\bar{\delta})E_{qj}^{'}\right| \le \sum_{j=1}^{n}\Gamma_{ij}\left|E_{qj}^{'}\right|, \tag{21}$$

where Γ_{ij} is some positive number.

Remark 1: We are not assuming that E_{fd} and $E_{qi}^{'}$ are bounded, but we are making an assumption that their rate of increase is bounded during the analysis of $\dot{E}_{qi}^{'}$. Thus, this assumption is a mild one.

Now let's analyze the bound of the interconnection terms $\left|\Delta_{i1}(.)\right|$. Based on (15), (16), and (21), it is easy to verify that there exist some positive constants A_{ij}, B_{ij}, C_{ij}, and D_{ij}, such that the following inequalities exist.

$$\begin{aligned}
&\left|(X_{qi} - X_{di})I_{di}I_{qi}\right| \le \sum_{j=1}^{n}A_{ij}E_{qj}^{'2},\\
&\left|E_{qi}^{'}\dot{I}_{qi}\right| \le \sum_{j=1}^{n}B_{ij}E_{qj}^{'2},\\
&\left|(X_{qi} - X_{di}^{'})\dot{I}_{di}I_{qi}\right| \le \sum_{j=1}^{n}C_{ij}E_{qj}^{'2},\\
&\left|(X_{qi} - X_{di}^{'})I_{di}\dot{I}_{qi}\right| \le \sum_{j=1}^{n}D_{ij}E_{qj}^{'2}.
\end{aligned} \tag{22}$$

We can thus conclude that $\left|\Delta_i(.)\right|$ is bounded according to

$$\left|\Delta_i(.)\right| \le \sum_{j=1}^{n}E_{ij}E_{qj}^{'2}, \tag{23}$$

where $E_{ij} = A_{ij} + B_{ij} + C_{ij} + D_{ij}$.

Define $x_{i1} = \delta_i$, $x_{i2} = \Delta\omega_i = \omega_i - \omega_s$, $x_{i3} = -\frac{\omega_s}{2H_i}$. ΔP_{ei}, $u_i = -\frac{\omega_s}{2H_iT_{d0i}^{'}}\Delta v_i$, and $k_i = -\frac{1}{T_{d0i}^{'}}$, then the above system model can be transformed into the following simplified system

$$\begin{cases}
\dot{x}_{i1} = x_{i2}\\
\dot{x}_{i2} = x_{i3}\\
\dot{x}_{i3} = k_ix_{i3} + u_i + \Delta_i(.).
\end{cases} \tag{24}$$

The output of the system is the power angle denoted as $y_i = x_{i1}$. Our objective is to make the system output track the desire set point, i.e., $\delta_i \to \delta_i^d$.

In (24), the definition of $\Delta_i(.)$ is different from that of (20). The bound of the new $\Delta_i(.)$ is given by

$$\begin{aligned}
\left|\Delta_i(.)\right| &\le \frac{\omega_s}{2H_{\min}T_{d0\min}^{'}}\left|P_{e0} - X_0\right|_{\max}\\
&\quad + \frac{\omega_s}{2H_{\min}}\sum_{j=1}^{n}E_{ij}E_{qj}^{'2}\\
&\le \delta_{i0} + \sum_{j=1}^{n}\delta_{ij}E_{qj}^{'2}.
\end{aligned} \tag{25}$$

4. CONTROLLER DESIGN

In this section, a NN based controller designs is proposed. The controller design is introduced using a theorem, and is described as follows.

First, consider the i-th subsystem. Define the filter error r_i as

$$r_i = [\Lambda_i^T \quad 1]^T x_i, \tag{26}$$

where $x_i = [x_{i1}, x_{i2}, x_{i3}]^T$ and $\Lambda_i = [\lambda_{i1}, \lambda_{i2}]^T$ is an appropriately chosen coefficient vector such that $x_i \to 0$ as $r_i \to 0$ (i.e., $s^2 + \lambda_{i2}s + \lambda_{i1} = 0$ is Hurwitz). Taking the derivative of r_i to get

$$\dot{r}_i = [0 \quad \Lambda_i^T]x_i + f_i(.) + u_i + \Delta_i(x) + d_i. \tag{27}$$

For subsystem without interconnection term $\Delta_i(x)$, the control signal u_i can be chosen as

$$u_i = -K_ir_i - [0 \quad \Lambda_i^T]x_i - f_i(.), \tag{28}$$

where $K_i > 0$ is the design parameter.

To compensate the effects of interconnection terms, NN are used here. According to the NN approximation theory, it can be concluded that there exists a NN such that

$$W_i^T\Phi_i(X_i) + \varepsilon_i = \sum_{j=1}^{n}E_{ji}E_{qi}^{'2}, \tag{29}$$

where $X_i = [E_{qi}^{'2}, 1]^T$ is the input vector to the NN, ε_i is the bounded NN approximation error given by $\left|\varepsilon_i\right| \le \varepsilon_{iM}$.

Thus, the actual control signal can be chosen as

$$u_i = -K_ir_i - [0 \quad \Lambda_i^T]x_i - f_i(.) - \mathrm{sgn}(r_i)\hat{W}_i^T\Phi_i(X_i). \tag{30}$$

The Lyapunov function for the i-th subsystem is chosen according to

$$V_i = \frac{1}{2} r_i^2 + \frac{1}{2} \tilde{W}_i^T \Gamma_i^{-1} \tilde{W}_i, \tag{31}$$

where $\tilde{W}_i$ is the weight estimation error defined as

$$\tilde{W}_i = \hat{W}_i - W_i \tag{32}$$

and $\Gamma_i > 0$ is another design parameter.

Taking the derivative of V_i to get

$$\begin{aligned} \dot{V}_i &= -K_i r_i^2 - |r_i| \hat{W}_i^T \Phi_i(X_i) + r_i \Delta_i(x) + \tilde{W}_i^T \Gamma_i^{-1} \dot{\tilde{W}}_i \\ &\le -K_i r_i^2 - |r_i| \hat{W}_i^T \Phi_i(X_i) + |r_i| \sum_{j=1}^{n} E_{ij} E_{qj}^{'\,2} + \tilde{W}_i^T \Gamma_i^{-1} \dot{\tilde{W}}_i. \end{aligned} \tag{33}$$

Thus the Lyapunov function for the overall system becomes

$$V = \sum_{i=1}^{n} V_i, \tag{34}$$

$$\begin{aligned} \dot{V}_i \le \sum_{i=1}^{n} \Bigg[& K_i r_i^2 - |r_i| \hat{W}_i^T \Phi_i(X_i) \\ & + |r_i| \sum_{j=1}^{n} E_{ij} E_{qj}^{'\,2} + \tilde{W}_i^T \Gamma_i^{-1} \dot{\tilde{W}} \Bigg]. \end{aligned} \tag{35}$$

Note that

$$\sum_{i=1}^{n} \sum_{j=1}^{n} E_{ij} E_{qj}^{'\,2} = \sum_{i=1}^{n} \sum_{j=1}^{n} E_{ji} E_{qi}^{'\,2}. \tag{36}$$

Thus

$$\begin{aligned} \dot{V} &\le \sum_{i=1}^{n} \begin{bmatrix} -K_i r_i^2 - |r_i| \hat{W}_i^T \Phi_i(X_i) + |r_i| W_i^T \Phi(X_i) \\ + |r_i| \varepsilon_i^M + \tilde{W}_i^T \Gamma_i^{-1} \dot{\tilde{W}}_i \end{bmatrix} \\ &\le \sum_{i=1}^{n} \Big[-K_i r_i^2 - |r_i| \tilde{W}_i^T \Phi_i(X_i) \\ &\qquad + \tilde{W}_i^T \Gamma_i^{-1} \dot{\tilde{W}}_i + |r_i| \varepsilon_{iM} \Big]. \end{aligned} \tag{37}$$

The weights updating rules is changed to

$$\dot{\hat{W}}_i = \Gamma_i |r_i| \Phi_i(X_i) - \alpha_i \Gamma_i \hat{W}_i. \tag{38}$$

Then (37) becomes

$$\dot{V} \le \sum_{i=1}^{n} (-K_i r_i^2 - \alpha_i \tilde{W}_i^T \hat{W}_i + |r_i| \varepsilon_{iM}). \tag{39}$$

Since

$$\begin{aligned} -\alpha_i \tilde{W}_i^T \hat{W}_i &\le -\alpha_i \tilde{W}_i^T (\tilde{W}_i + W_i) \\ &\le -\alpha_i |\tilde{W}_i|^2 + \alpha_i |\tilde{W}_i| |W_i| \le -\frac{\alpha_i}{2} |\tilde{W}_i|^2 + \frac{\alpha_i}{2} W_{i\max}^2 \end{aligned} \tag{40}$$

and

$$\varepsilon_i^M |r_i| \le \frac{r_i^2}{2} + \frac{1}{2} \varepsilon_{iM}^2, \tag{41}$$

thus,

$$\dot{V} \le \sum_{i=1}^{n} [-(K_i - \frac{1}{2}) r_i^2 - \frac{\alpha_i}{2} |\tilde{W}_i|^2 + \frac{\alpha_i}{2} W_{i\max}^2 + \frac{1}{2} \varepsilon_{iM}^2]. \tag{42}$$

For simplification, define $\delta = \sum_{i=1}^{n} \frac{\alpha_i W_{i\max}^2 + \varepsilon_{iM}^2}{2}$.

If the selection of design parameters K_i and α_i, such that $K_i > \gamma + \frac{1}{2}$, and $\alpha_i \ge \gamma \lambda_{\max}(\Gamma_i^{-1})$, then we get

$$\begin{aligned} \dot{V} &\le \sum_{i=1}^{n} \left[-(K_i - \frac{1}{2}) r_i^2 - \frac{\alpha_i}{2} |\tilde{W}_i|^2 \right] + \delta \\ &\le -\gamma \sum_{i=1}^{n} \left[r_i^2 + \tilde{W}_i^T \Gamma_i^{-1} \tilde{W}_i \right] + \delta \le -\gamma V + \delta. \end{aligned} \tag{43}$$

Theorem 1: Consider the closed loop system consisting of system (24), the control signal (30), and the NN weight updating laws (38). For bounded initial conditions, all signals in the closed loop system remain uniformly ultimately bounded, and the system states x and NN weight estimates $\hat{W}$ eventually converge to a compact set Ω.

$$\Omega = \left\{ r, \hat{W} \,\middle|\, V < \frac{\delta}{\gamma} \right\} \tag{44}$$

Proof: From (44), we can see that if r_i and $\tilde{W}_i$ are outside of the compact set defined as (45), then $\dot{V}$ will remain negative definite until the systems state and the weight estimate errors enter the Ω. Thus, r_i and $\tilde{W}_i$ are uniformly ultimately bounded. Furthermore, since W_i exist and are bounded, then $\hat{W}_i$ are also bounded. Considering (26) and the boundedness of r_i, we can conclude that x_i is bounded. Using (28), we conclude that control signal u is also bounded.

Thus, all signals in the closed loop system remain bounded, and the system state vector x, and NN weight estimates $\hat{W}_i$ eventually converge to a compact set Ω [25].

Remark 2: In the proposed weight updates, persistency of excitation condition is not required. Weight updates using (38) is similar to σ-modification in the standard adaptive control.

Remark 3: The weights of the hidden layer are randomly chosen initially between 0 and 1, and fixed, therefore, not adapted. The initial weights of the output layer are just set to zero and then adapted

online according to (38). There is no preliminary off-line learning phase, and stability will be provided by the outer tracking loop until the NN learns. This is a significant improvement over other NN control techniques where one must find some initial stabilizing weights, generally a difficult task for complex nonlinear systems over a wide range of operating conditions.

5. SIMULATION STUDIES

The proposed decentralized NN controller design is tested with the WECC 3-machine 9-bus system, which is shown in Fig. 2. The parameters of the system are borrowed from [23]. For convenience, the parameters of the generator and excitation systems, and the transmission lines are listed in Tables 1-2, respectively.

The design parameters for the three generators are the same, and chosen as Λ_i=[4, 4], K_i=2, Γ_i=2, α_i=2. Each neural network is selected to have ten hidden neurons in the hidden layer, and logarithmic sigmoid transfer functions.

The proposed decentralized controller is evaluated under the following two operating conditions.

Test 1: A 200ms line loss. Line 5-7 was disconnected for 200ms at 1sec and then recovered at 1.2sec.

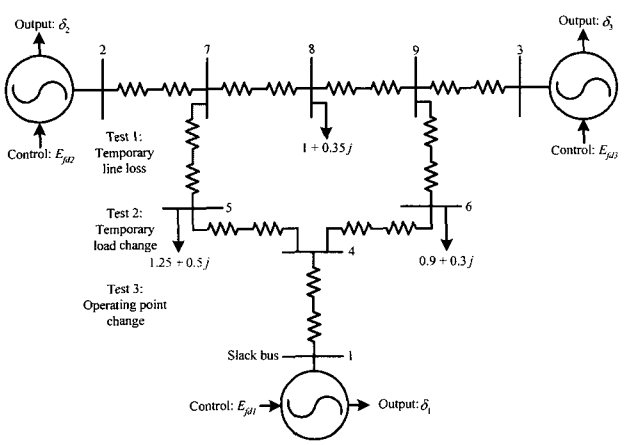

Fig. 2. Configuration of the WECC 3-machine power system.

Table 1. Parameters of the generators.

Parameters	Machine 1	Machine 2	Machine3
H (sec)	23.64	6.4	3.01
X_d (pu)	0.146	0.8958	1.3125
$X_d^{'}$ (pu)	0.0608	0.1198	0.1813
X_q (pu)	0.0969	0.8645	1.2578
$T_{d0}^{'}$ (sec)	8.96	6.0	5.89
T_a (sec)	0.2	0.2	0.2
K_a (pu)	20	20	20

Table 2. Parameters of the transmission lines.

Bus i	Bus j	R_{ij}	X_{ij}	B_{ij}
1	4	0	0.0576	0
2	7	0	0.0625	0
3	9	0	0.0586	0
4	5	0.01	0.085	0.088
4	6	0.017	0.092	0.079
5	7	0.032	0.161	0.153
6	9	0.039	0.17	0.179
7	8	0.0085	0.072	0.0745
8	9	0.0119	0.1008	0.1045

Test 2: A 200ms load change. Load connected to bus 5 was doubled at 1sec and then changed back at 1.2sec.

For each of the three cases, the proposed controller is compared with the case without control, and the case under conventional controls. This idea is illustrated in Fig. 3, where there are three positions for the switch to connect the NNDC (Neural Network based Decentralized Controller), the conventional controllers consisted of an AVR and a CPSS, and the ground (without control). The model of the voltage regulator and the configuration of CPSS are shown in (45) and Fig. 4, respectively.

$$T_{ai}\dot{E}_{fdi} = -E_{fdi} + K_{ai}(V_{refi} - V_i + V_{pssi}) \tag{45}$$

Usually the two lead-lag compensator blocks in CPSS are identical, which means T_1=T_3, T_2=T_4, thus there are five tunable parameters for each CPSS, i.e., T_1, T_2, T_5, T_6, and K_{pss}. If equipping all the three generators with CPSSs, there will be 15 design parameters in total. Improper selection of the design parameters will result in interaction between the CPSSs that will deteriorate the dynamic performance of the power system. Thus, the 15 parameters need to be tuned together, which is a very difficult task. To obtain a convincing comparison, the proposed controller design should be compared to the best possible performance of the CPSS. To do that, Particle Swarm Optimization (PSO) is used in this paper,

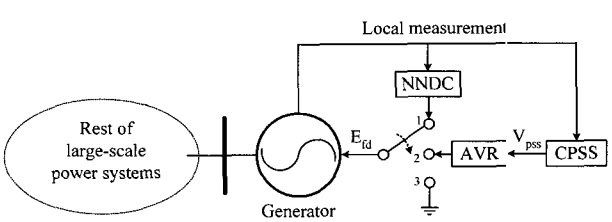

Fig. 3. Generator controlled with different controllers.

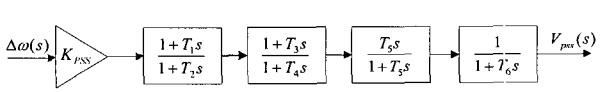

Fig. 4. Structure of CPSS suggested by IEEE Std. 421.5 [26].

trying to find the best set of CPSS parameters.

PSO is one of the latest evolutionary computation techniques that is simple in concept, easy to implement and computationally efficient [27]. The updating rules of PSO are given in (46).

$$\begin{aligned} V_{new} &= w \times V_{old} + c_1 \times rand_1 \times (P_{best} - P_{old}) \\ &\quad + c_2 \times rand_2 \times (L_{best} - P_{old}), \\ P_{new} &= P_{old} + V_{new}, \end{aligned} \tag{46}$$

where V_{new} is the new velocity vector calculated for each particle; V_{old} is the velocity vector from the previous iteration; P_{new} is the new position vector calculated for each particle; P_{old} is the position vector of the particle from the previous iteration; W is the inertia weight constant; c_1 and c_2 is the acceleration constant; and *rand* is the generates a uniform random value between [0 1]. Detailed description of the algorithm can be found in [27].

According to literature and IEEE recommendation, the ranges of the five parameters are set as $T_1 \in [0.1 \quad 1]$, $T_2 \in [0.01 \quad 0.1]$, $T_5 \in [1 \quad 10]$, $T_6 \in [0.001 \; 0.01]$, and $K_{PSS} \in [0.01 \quad 0.1]$. The population size is chosen to be 10. The values for the positive constant w, c_1, and c_2 are 0.8, 2, and 2 respectively.

To evaluate a particle (a vector of the 15 CPSS parameters), the system is simulated with the set of parameters for some kind of fault. Before the fault is applied, the system is running stable. For the dynamic performance evaluation purpose, only the post-fault response is considered. The sampling time is 0.01 sec. 900 samples data are collected for each candidate solution, which means 9-sec performance after the fault is applied. Then the cost is calculated from the simulation data according to (47).

$$\cos t = \sum_{i=1}^{n} t(i) \cdot |\Delta\omega(i)|, \tag{47}$$

where n is the number of sampled data (900 for our case), $t(i)$ is the time of the i^{th} sample data, and $\Delta\omega(i) = \omega(i) - \omega_s$ is the speed deviation at time $t(i)$. The multiplication of $t(i)$ and $|\Delta\omega(i)|$ gives faster damping a lower cost.

For each test, the optimization process terminated after 20 iterations. Table 3 shows the obtained optimal sets of CPSS parameters corresponding to the two tests.

From Table 3, it can be seen that the three sets of CPSS parameters optimized for the three operating conditions are different. Simulation studies also show that a CPSS optimized for an operating condition may not work satisfactorily for another operating condition. Table 3 explains why the tuning of CPSS parameters is difficult. To present a convincing comparison, the proposed NN-based controller design with fixed

Table 3. Optimal CPSS parameters tuned by PSO.

		K_{PSS}	T_1	T_2	T_5	T_6
CPSS1 (Test1)	*CPSS1-1*	0.0350	0.9209	0.0961	9.7246	0.0012
	CPSS1-2	0.0109	0.9102	0.0634	9.9781	0.0071
	CPSS1-3	0.0662	0.2831	0.0183	9.2696	0.0099
CPSS2 (Test2)	*CPSS2-1*	0.0974	0.1278	0.0107	9.6142	0.0041
	CPSS2-2	0.0997	0.1773	0.0101	9.7898	0.0015
	CPSS2-3	0.0915	0.2930	0.0128	1.0140	0.0012

design parameters is compared with the best CPSSs corresponding to the two tests. Simulation results are provided in Figs. 5-17.

5.1. 200ms line loss test

Simulation results for the three cases (without control, with optimized CPSS, and the proposed NNDC) are provided in Figs. 5-12. Since the ranges of the responses for the three cases are different, simulation results are plotted separately. In the following figures, G1, G2, and G3 stand for the responses of three generators respectively. The unit of the speed is radian per second (rad/sec). The units for the terminal voltage and control signal are per unit (p.u.).

5.1.1 Without excitation control

From Figs. 5 and 6, oscillations of different modes can be observed. These oscillations are caused by the

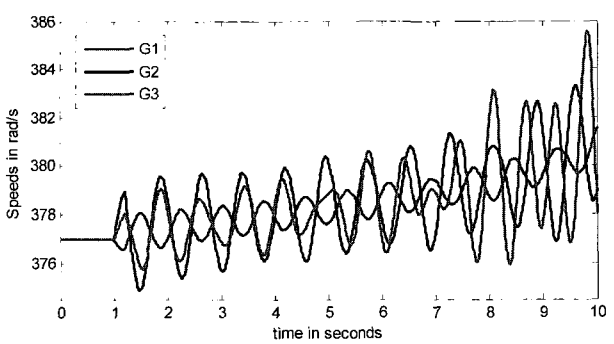

Fig. 5. Speed deviation responses when there is no excitation control.

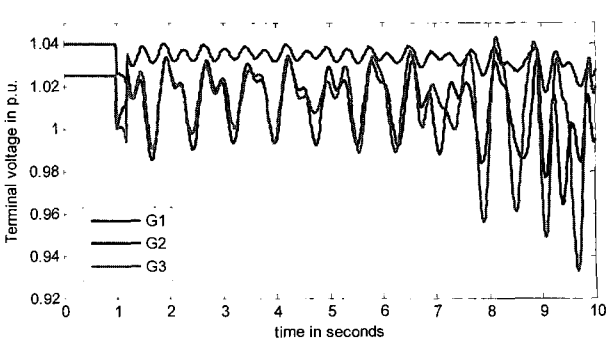

Fig. 6. Terminal voltage responses when there is no excitation control.

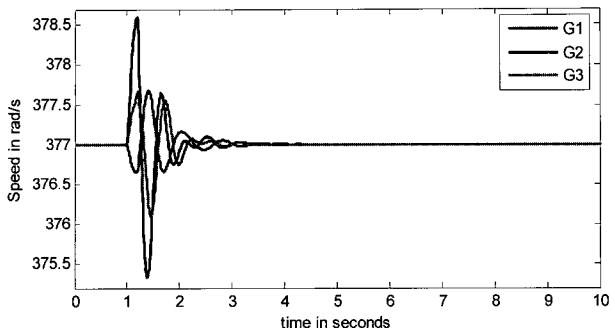

Fig. 7. Speed deviation responses with CPSS1.

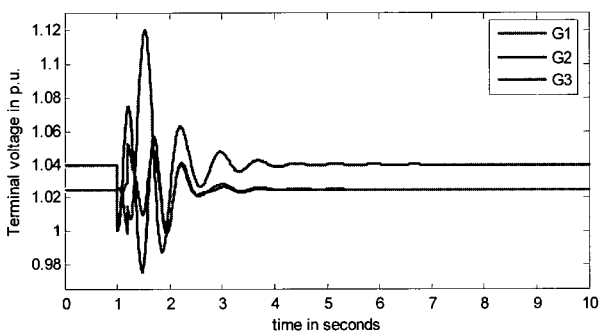

Fig. 8. Terminal voltage responses with CPSS1.

interactions between generators. It is important to note that the system will settle down to some operating point eventually, but the oscillations will persist for a long time, which is harmful for the transient stability of power systems and even limits the power transfer capability.

5.1.2 With the optimized CPSS1

Figs. 7 and 8 are simulation results for CPSS1, which is optimized specifically for Test 1. Form the simulation results it can be seen that the oscillations were efficiently damped out. But the speed oscillation is between the range of 375.5 rad/sec and 378.5 rad/sec. If we compare it with the response of NNDC in Fig. 10, we can see that the NNDC can provide a much better damping by damping the oscillation within the range of 376.7 rad/sec and 377.3 rad/sec.

5.1.3 With neural networks based decentralized control

Simulation results of NNDC for Test 1 are provided in Figs. 9-12.

Usually, damping control will have a bad impact on the voltage control. From Fig. 10, it can be seen that the impact of the damping control on the terminal voltage response is acceptable. It has been proved that all the signals in the closed loop system are uniformly ultimately bounded. The weights and control signals responses confirmed the previous analysis. Unlike single machine power system, where the magnitude constraint of control signals can be modeled as

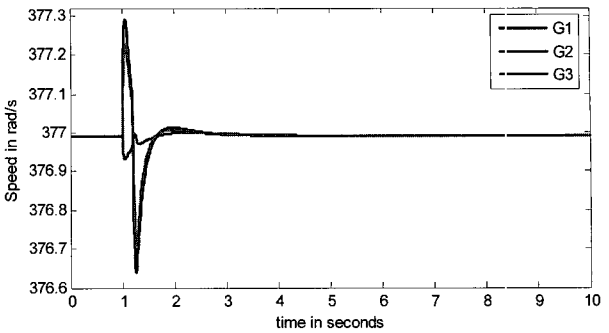

Fig. 9. Speed deviation responses with the NNDC.

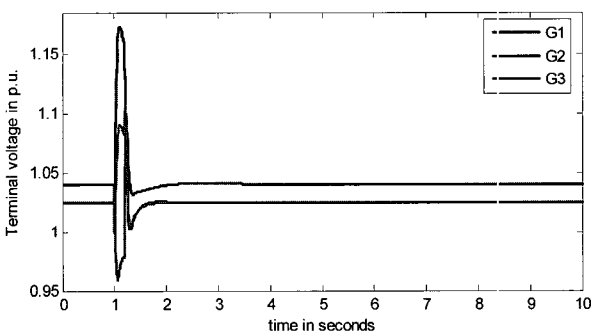

Fig. 10. Terminal voltage responses with the NNDC.

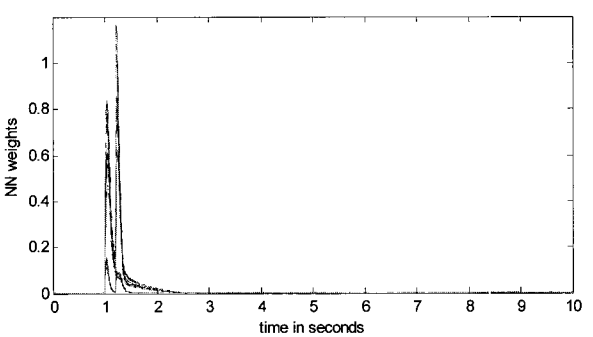

Fig. 11. Neural network weights updating process of the NNDC.

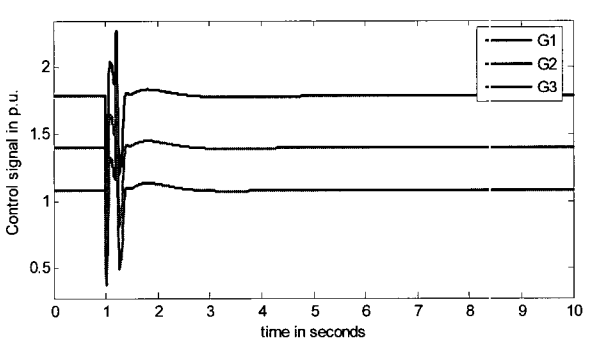

Fig. 12. Control signal responses with the NNDC.

saturation nonlinearities and included in the stability analysis [16,18], it is very difficult to do this for decentralized controls. Fortunately, the magnitude of the control signals can be decreased by proper selection of the design parameters. Of course, trying

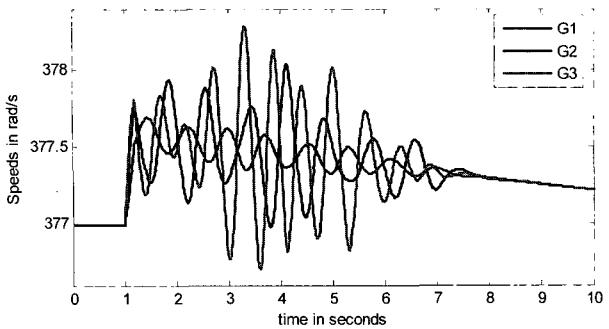

Fig. 13. Speed deviation responses when there is no excitation control.

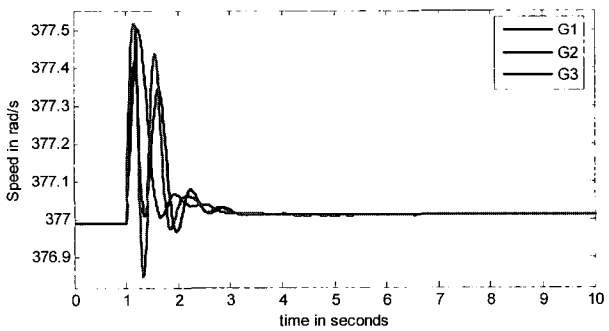

Fig. 14. Speed deviation responses with CPSS2.

to do this will impact the control performance. Even though, the performance will still be much better than that of conventional controllers.

5.2. 200ms load change test

Simulation results for Test 2 are provided in Figs 13-17. Again, the responses for the three cases are plotted in separate figures.

5.2.1 Without excitation control

Similar to Test 1, oscillations of different modes can be observed in Fig. 13. If the simulation program is run for longer time, we will see that the speeds finally converge to the equilibrium point, but it will take too long time.

5.2.2 With the optimized CPSS2

From Fig. 14, it can be seen that the optimized CPSS can provide good damping compared to the case of without stabilizing control. It should be noted that the CPSS parameters used for this test are different from Test1. The purpose of doing this is to compare the NNDC with the best possible performance of CPSS. During practical operations, parameter settings of CPSS need to balance all operating conditions under consideration. That indicates that its performance for a particular operating condition will not be as good as this optimized one.

5.2.3 With neural networks based decentralized control

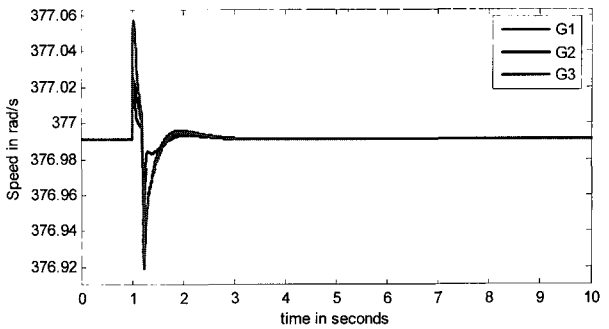

Fig. 15. Speed deviation responses with the NNDC.

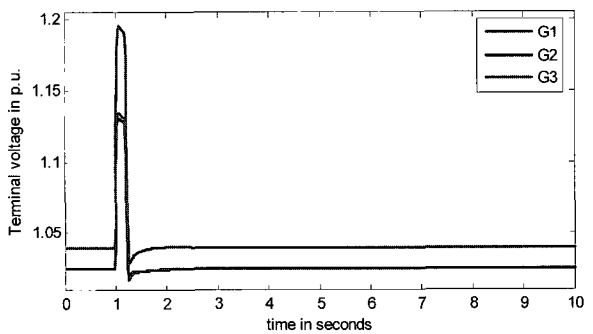

Fig. 16. Terminal voltage responses with the NNDC.

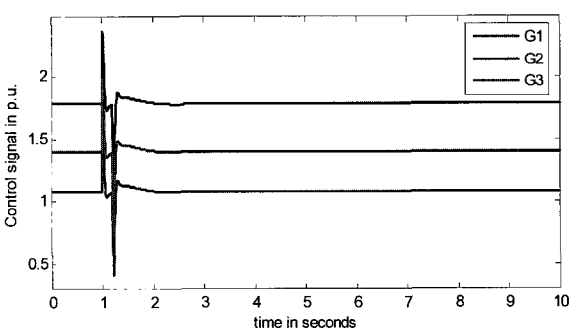

Fig. 17. Control signal responses with the NNDC.

Figs. 15-17 are simulations results for the proposed decentralized controllers. The design parameters of NNDC for this test are the same as Test 1.

From these figures, it can be seen that the NNDC can adapt to operating condition changes, and provide much better performance than the optimized conventional controllers.

6. CONCLUSIONS

This paper introduced a new neural networks based decentralized controller designs for the excitation control of multimachine power systems. Though only local measurable/calculatable signals are used to calculate the subsystem control input, coordination of the subsystem control activities and the transient performance are guaranteed. Simulation results demonstrate that the proposed controller provides

good performance, and outperforms the optimized conventional design methods in many aspects. Future work includes the consideration of more practical power system models.

REFERENCES

[1] Q. Lu and Y. Sun, "Nonlinear stabilizing control of multimachine power systems," *IEEE Trans. on Power Systems*, vol. 4, no. 1, pp. 236-241, February 1989.

[2] J. W. Chapman, M. D. Ilic, C. A. King, L. Eng, and H. Kaufman, "Stabilizing a multimachine power system via decentralized feedback linearizing excitation control," *IEEE Trans. on Power Systems*, vol. 8, no. 3, pp. 830-839, 1993.

[3] S. Jain, F. Khorrami, and B. Fardanesh, "Adaptive nonlinear excitation control of power systems with unknown interconnections," *IEEE Trans. on Control Systems Technology*, vol. 2, no. 4, pp. 436-446, 1994.

[4] H. Jiang, H. Cai, J. F. Dorsey, and Z. Qu, "Toward a globally robust decentralized control for large-scale power systems," *IEEE Trans. on Control Systems Technology*, vol. 5, no. 3, pp. 309-319, May 1997.

[5] Y. Guo, D. J. Hill, and Y. Wang, "Nonlinear decentralized control of large scale power systems," *Automatica*, vol. 36, no. 9, pp. 1275-1289, 2000.

[6] Z. Xi, G. Feng, D. Cheng, and Q. Lu, "Nonlinear decentralized saturated controller design for power systems," *IEEE Trans. on Control Systems Technology*, vol. 11, no. 4, pp. 539-547, July 2003.

[7] L. Jiang, Q. H. Wu, and J. Y. Wen, "Decentralized nonlinear adaptive control of multimachine power systems via high-gain perturbation observer," *IEEE Trans. on Circuit Systems-I*, vol. 51, no. 10, pp. 2052-2059, October 2004.

[8] H. E. Psillakis and A. T. Alexandridis, "A new excitation control for multimachine power systems I: Decentralized nonlinear adaptive control design and stability analysis," *International Journal of Control, Automation, and Systems*, vol. 3, no. 2, pp. 278-287, June 2005.

[9] H. E. Psillakis, A. T. Alexandridis, "A new excitation control for multimachine power systems II: Robustness and disturbance attenuation analysis," *International Journal of Control, Automation, and Systems*, vol. 3, no.2, pp. 288-295, June 2005.

[10] K. I. Jung, K. Y. Kim, T. W. Yoon, and G. Jang, "Decentralized control for multimachine power systems with nonlinear interconnections and disturbances," *International Journal of Control, Automation, and Systems*, vol. 3, no. 2, pp. 270-277, June 2005.

[11] S. Huang, K. K. Tan, and T. H. Lee, "Decentralized control design for large-scale systems with strong interconnections using neural network," *IEEE Trans. on Automatic Control*, vol. 48, no. 5, pp. 805-810, 2003.

[12] J. T. Spooner and K. M. Passino, "Decentralized adaptive control of nonlinear systems using radial basis neural networks," *IEEE Trans. on Automatic Control*, vol. 44, pp. 2050-2057, November 1999.

[13] W. Liu, S. Jagannathan, D. C. Wunsch, and M. L. Crow, "Decentralized neural network control of a class of large-scale systems with unknown interconnections," *Proc. of the 43rd Conf. Decision and Control*, Atlantis, Bahamas, vol. 5, pp. 4972- 4977, December 14-17, 2004.

[14] W. Liu, G. K. Venayagamoorthy, and D. C. Wunsch II, "Design of an adaptive neural network based power system stabilizer," *Neural Networks*, vol. 16, no. 5-6, pp. 891-898, July 2003.

[15] W. Liu, G. K. Venayagamoorthy, and D. C. Wunsch II, "A heuristic dynamic programming based power system stabilizer for a turbogenerator in a single machine power system," *IEEE Trans. on Industry Applications*, vol. 41, no. 5, pp. 1377-1385, September 2005.

[16] W. Liu, J. Sarangapani, G. K. Venayagamoorthy, D. C. Wunsch II, and M. L. Crow, "Neural network stabilizing control of single machine power system with control limits," *Proc. of the International Joint Conf. Neural Networks*, Budapest, Hungary, pp. 1823-1828, July 25-29, 2004.

[17] W. Liu, J. Sarangapani, G. K. Venayagamoorthy, D. C. Wunsch II, M. L. Crow, L. Liu, and D. A. Cartes, "Neural network based decentralized controller designs for large scale power systems," *Proc. of the 22nd IEEE International Symp. Intelligent Control*, Singapore, October 2007.

[18] W. Liu, G. K. Venayagamoorthy, J. Sarangapani, D. C. Wunsch II, M. L. Crow, L. Liu, and D. A. Cartes, "Comparisons of an adaptive neural network based controller and an optimized conventional power system stabilizer," *Proc. of the 16th IEEE Conf. Control Applications*, Singapore, October 2007.

[19] A. R. Baron, "Universal approximation bounds for superposition of a sigmoid function," *IEEE Trans. on Information Theory*, vol. 39, no. 3, pp. 930-945, 1993.

[20] N. Sadegh, "A perceptron network for functional identification and control of nonlinear systems," *IEEE Trans. on Neural Networks*, vol. 4, pp. 1823-1836, 1992.

[21] B. Igelnik and Y.-H. Pao, "Stochastic choice of basis functions in adaptive function approximation and the functional-link net," *IEEE Trans. on Neural Networks*, vol. 6, no. 6, pp. 1320-1329, November 1995.

[22] F. L. Lewis, S. Jagannathan, and A. Yesildirek, *Neural Network Control of Robot Manipulators and Nonlinear Systems*, Taylor and Francis, 1999.

[23] P. W. Sauer and M. A. Pai, *Power System Dynamics and Stability*, Prentice Hall, 1997.

[24] Y. Wang, D. J. Hill, and G. Guo, "Robust decentralized control for multimachine power systems," *IEEE Trans. on Circuits and Systems*, vol. 45, no. 3, pp. 271-279, 1998.

[25] S. S. Ge and C. Wang, "Direct adaptive NN control of a class of nonlinear systems," *IEEE Trans. on Neural Networks*, vol. 13, no. 1, pp. 214-221, 2002.

[26] IEEE, *Recommended Practice for Excitation System Models for Power System Stability Studies*, IEEE Std. 421.5-1992, 1992.

[27] J. Kennedy and R. Eberhart, "Particle swarm optimization," *Proc. of IEEE International Conf. Neural Networks*, vol. IV, pp. 1942-1948, 1995.

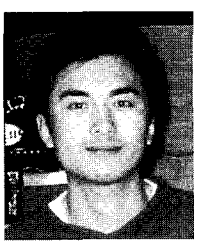

Wenxin Liu received the B.S. degree in Industrial Automation and M.S. degree in Control Theory and Applications in 1996 and 2000 respectively both from the Northeastern University of China, and the Ph.D. degree from the University of Missouri at Rolla in 2005. He joined Center for Advanced Power Systems of Florida State University in 2005 as a Postdoctoral fellow and now an Assistant Scholar Scientist. His research interests include adaptive and neural network control, power systems, and applications of computational intelligence. He is a Member of IEEE and Sigma Xi.

Sarangapani Jagannathan is a Professor and Site Director for the National Science Foundation Industry/ University Cooperative Research Center on Intelligent Maintenance Systems at the University of Missouri at Rolla. He received the B.S. degree from the College of Engineering, Guindy at Anna University, Madras, India, in 1987, the M.S. degree from the University of Saskatchewan, Saskatoon, Canada, in 1989, and the Ph.D. degree from the University of Texas, San Antonio, in 1994, all in Electrical Engineering. He has coauthored more than 170 refereed conference and reviewed journal articles and several book chapters and three books. Currently, he holds 17 patents and several are in process. His research interests include adaptive and neural network control, computer/ sensor/communication networks, prognostics, and autonomous systems/robotics.

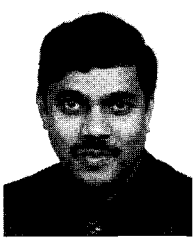

Ganesh Kumar Venayagamoorthy is an Associate Professor of Electrical and Computer Engineering and the Director of the Real-Time Power and Intelligent Systems Laboratory at the University of Missouri at Rolla. He received the B.Eng. degree in Electrical and Electronics Engineering from Abubakar Tafawa Balewa University, Bauchi, Nigeria, in 1994 and the M.Sc.Eng. and Ph.D. degrees in Electrical Engineering from the University of Natal, Durban, South Africa, in 1999 and 2002, respectively. He has published 2 edited books, 3 book chapters, 40 refereed journals papers and 190 refereed international conference proceeding papers. He has attracted close to US $3 million in research funding to date. His research interests are in development and applications of computational intelligence for power systems stability and control, FACTS devices and alternative sources of energy.

Li Liu received the B.S. degree in Mechanical Engineering from TongJi University, Shanghai, China in 1997, the M.S. degree in the same field from Shanghai Jiao Tong University, Shanghai, China in 2000. She then joined General Motors (Shanghai) as a Product Engineer and worked there for two years. In 2002, she entered Florida State University, where she received the Ph.D. degree in Dynamics and Controls, Mechanical Engineering in 2006. Currently, she is a Postdoctoral Fellow with Center for Advanced Power Systems. Her research interests are condition based maintenance, fault detection, diagnosis, nonlinear system identification and controls for electric motors.

Donald C. Wunsch II is the Mary K. Finley Distinguished Professor of Computer Engineering and the Director of Applied Computational Intelligence Laboratory at the University of Missouri at Rolla. He received the B.S. degree in Applied Mathematics from the University of New Mexico, Albuquerque, and the M.S. degree in Applied Mathematics and the Ph.D. degree in Electrical Engineering from the University of Washington, Seattle. He has well over 200 publications and has attracted more than $5 million in research funding. He served as General Chair for IJCNN'03 and 2005 President of the International Neural Networks Society. He is a Fellow of IEEE. His research interests include adaptive critic designs, neural networks, fuzzy systems, surety, nonlinear adaptive control, intelligent agents, and applications.

Mariesa L. Crow is the F. Finley Distinguished Professor of Electrical Engineering and the Director of Energy Research and Development Center at the University of Missouri at Rolla. She received the BSE in Electrical Engineering from the University of Michigan and the Ph.D. in Electrical Engineering from the University of Illinois at Urbana/Champaign. She has authored a book, several book chapters, over 100 technical articles, and has participated in research projects totaling over $11 million in the past 10 years. Her area of professional interest is power electronics applications to bulk power transmission systems analysis and security.

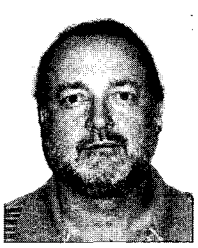

David A. Cartes is an Associate Professor of Mechanical Engineering and an Associate Director of Center for Advanced Power Systems (CAPS) at Florida State University (FSU). In 1994, he completed a 20-year U.S. Navy career with experience in operation, conversion, overhaul, and repair of complex marine propulsion systems. He joined FSU in January 2001, after receiving the Ph.D. in Engineering Science from Dartmouth College. He heads the Power Controls Lab at CAPS. He is a Member of the American Society of Naval Engineers and a Senior Member of IEEE. His research interests include distributed control and reconfigurable systems, real-time system identification, and adaptive control.